Journal of Modern Materials
ISSN: 2456-4834
Volume 10, Issue 1, pp. 3-10, 2023
DOI: https://doi.org/10.21467/jmm.10.1.3-10

RESEARCH ARTICLE

The Influence of Preparation Parameters on Structural and Optical Properties of N-Type Porous Silicon

K. M'hammedi[1, 2 *], N. Gabouze[1]

[1]Couches Minces, Surfaces et Interfaces' Division – Centre de Recherche en Technologie des Semi-conducteurs pour l'Energétique (CRTSE), 02 Bd. Frantz Fanon, B.P. 140, Alger 7-merveilles, Algiers, Algeria
[2]Laboratoire surfaces, Interfaces et couches minces, Faculté des Sciences, Département de Physique, Université Blida 1

[*]Corresponding author's e-mail: kawther_mhammedi@hotmail.fr
Received: 30 September 2022 / Revised: 09 January 2023 / Accepted: 16 January 2023 / Published: 05 March 2023

ABSTRACT

In this paper, we describe the formation of macroporous silicon (MPS) formed anodically polarized on n type Si (100) substrates at a constant current density under front side illumination using two electrolytes, HF/Ethanol and HF/Ethanol/H_2O_2. The effect of adding H_2O_2 in the solution on the resulting pores were investigated by scanning electron microscopy (SEM), infrared spectroscopy (FTIR), contact angle measurements and UV-vis spectrophotometry. The results showed that for the anodization conditions the MPS formed in peroxide based (H_2O_2)/HF/Ethanol solution exhibited structures with larger pore size and different pore morphologies depending on the etching time than those formed in HF/Ethanol. The pore density and the pore size of the MPS samples increased with the etching time. The infrared absorption spectrum (FTIR) carried out on the freshly prepared sample indicates that the MPS contains Si-H_x bonds which decrease with increasing the etching time. Finally, measurements of contact angle indicate that the formed MPS samples are highly hydrophobic.

Keywords: Macroporous Silicon, Illumination, Oxidant H_2O_2.

1 Introduction

Since the discovery of its luminescence properties at room temperature in 1990s, porous silicon PSi has known a great interest over the three last decades mainly due to its several potential applications as capacitors [1], membrane (pump of particles) [2], solar cell [3], Metallic barcodes[4] , gas sensing [5] fuel cell [6] etc. Porous silicon is classified according to its "pore size". According to the IUPAC nomenclature for porous materials [7], structures with a pore width below two nanometers are called microporous, then mesoporous for sizes under 50 nm, and macroporous for pore diameters larger than 50 nm. Macroporous silicon (MPS) is a novel material described as such in the early 1990s by Lehmann et al. in their pioneering works [8]–[10] which invented an electrochemical etching process to produce arrays of ordered macropores in silicon [6]. Since its first description, MPS has attracted great interest, and it has been suggested for many applications in several fields such as electronics [11], optics [5], photonics [12] solar cells [13] , and even energy storage [14] fuel cells [6] or catalysis [15] Several methods for the fabrication of ordered MPS have been used such as reactive ion etching, stain etching [16],metal assisted etching [17], direct laser writing (DLW) [18], lithographic methods (layer-by-layer [19], interference lithography [20], block copolymer [21]) and glancing angle deposition [22] However, the electrochemical etching of silicon remains one of the most important and versatile fabrication methods. In this method, the MPS layer is formed on the crystalline silicon (c-Si) by anodic electrochemical etching in aqueous hydrofluoric (HF) solution [23]. Anodic oxidation of silicon is connected with the consumption [10] of holes at the surface. On n-type Si holes can be generated by illumination of the surface (front-side or back surface). However, few results are available on macropores formed under front side illumination [24], [25] One advantage of the anodization method is the possibility

Copyright © 2023. The Author(s). Published by AIJR Publisher.
This is an open access article under Creative Commons Attribution-NonCommercial 4.0 International (CC BY-NC 4.0) license, which permits any non-commercial use, distribution, adaptation, and reproduction in any medium, as long as the original work is properly cited.

to produce ordered pore arrays with defined diameters and lengths. In addition, the pore diameters can be adjusted between a few hundred nanometers and several micrometers. However, it is known that the morphology of the pore obtained is dependent on several properties of the silicon substrate such as doping level and type, resistivity, and orientation, the composition of the electrolyte (organic, inorganic, and concentration), and external parameters such as temperature, voltage and illumination.

In this work, HF based electrolytes containing an oxidant (H_2O_2) are used to fabricate macropores considerably faster. The effect of the oxidant and etching time on structural, morphological and optical properties of n-type MPS has been studied. The results have been compared to those obtained on macropores achieved in electrolyte free H_2O_2.

2 Materials and Methods

N-type czochralski Si (100) single side polished silicon wafers with a thickness of 0.45 mm were used in this experiment. The n-Si wafers were phosphorus doped with a resistivity of 1 – 10 Ω.cm were commercially available from Wacker (Germany). All of the substrates were cut in a circular shape with a diameter of 1 cm. An ohmic contact was provided by an In-Ga eutectic at the back side of the sample. The silicon samples were etched in a standard photoelectrochemical cell in Teflon and connected to a Potensiostat–Galvanostat (VMP3-615 Biologic) by using two-electrode configuration where the Pt wire and Si sample were chosen to be cathode and anode, respectively. During the photoelectrochemical etching process, the sample was under frontal illumination with a 50 W Tungsten-Halogen lamp controlled by a stabilized dc power supply. Prior to the etching process, the samples were cleaned to remove any contamination on the surface. Two types of solution were prepared as electrolyte. The first electrolyte was a mixture of (48%) HF and (95%) ethanol (1/4 by Vol) ratio to prepare porous silicon samples for 30 min. The second electrolyte composed of (48%) HF/ (95%) ethanol/ (30%) H_2O_2 with (1/4/1 by Vol) ratio was used to prepare porous Si for different etching times (10, 20 and 30 min). The anodization current density was fixed in the range 4-20 mA/cm^2. After the etching process, the achieved macroporous samples were rinsed with ethanol and dried by nitrogen.

The morphological properties of MPS samples were studied by JOEL (JSM7_7610F PLUS) scanning electron microscope (SEM). For chemical analyses, Fourier Transform Infrared (FT-IR) spectroscopy was conducted using (Thermo Nicolet Nexus 870 ESP FT-IR) spectrometer. The porosity of porous samples was determined by a gravimetric method. The contact angle measurements of MPS were performed using a GBX Digidrop contact angle meter controlled by Visiodrop standard software. Reflectance measurements of the prepared samples were performed by spectrophotometry UV-Vis-Nir (Cary 500 scan VARIAN) in the range 400-2500 nm.

3 Results and discussion

3.1 Effect of electrolyte

Figure 1 shows the SEM surface images of Si etched in HF/Ethanol (sample a) and Si etched in HF/Ethanol/H_2O_2 (sample b) top view after etching under front side illumination for 30 min.

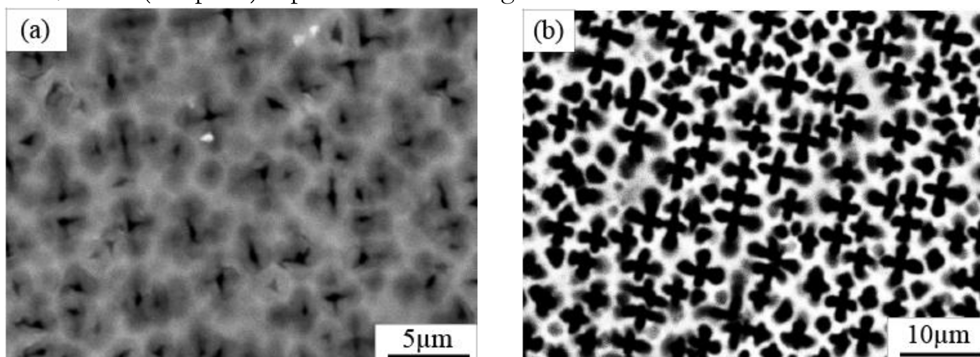

Figure 1: *SEM images for MPS with etching time of 30 min for different samples (a) without H_2O_2 (b) with H_2O_2.*

It clearly shows that the pore size formed in HF/ H_2O_2 is larger than without H_2O_2. On the other hand, the samples obtained with hydrogen peroxide show the bigger pore diameters. This is indicative that the peroxide promotes the etching in the edges of the pores as can be seen in the SEM images, as suggested by F. Severiano et al. [26]. The plan SEM view of sample (a) shows narrow pores with randomly distribution, which reduces pore density of this sample. In addition, significant changes of pore morphology are observed in sample (b), a four branch shaped pores with larger pore size and high porous density which are uniform across the whole surface. Moreover, Lu *et al.* [27]have shown that the addition of a strong (H_2O_2) oxidant into the electrolyte HF/Ethanol accelerates the oxidation process on p-type silicon and shortens the overall reaction time to speed up the etching process. The morphological observation indicated that the incorporation of H_2O_2 in the electrolyte increased the pore diameter [27].

Moreover, the pore density of sample (a) appears higher than on sample (b). This could be the result of successful dissolution of H_2O_2, which raises the pH of the solution and aids in the termination of Si-H bonds, resulting in a perfect Si surface [28] and, as a result, an increase in the size of the pores is observed.

3.2 Effect of etching time

Figure 2 shows the SEM images of MPS top view after etching under front side illumination for 10, 20 and 30 min. It is clearly observed that the geometry of the pore evolves with increasing etching time. The surface morphology of sample (a) has cubic (square) shaped macropores with a low pore density.

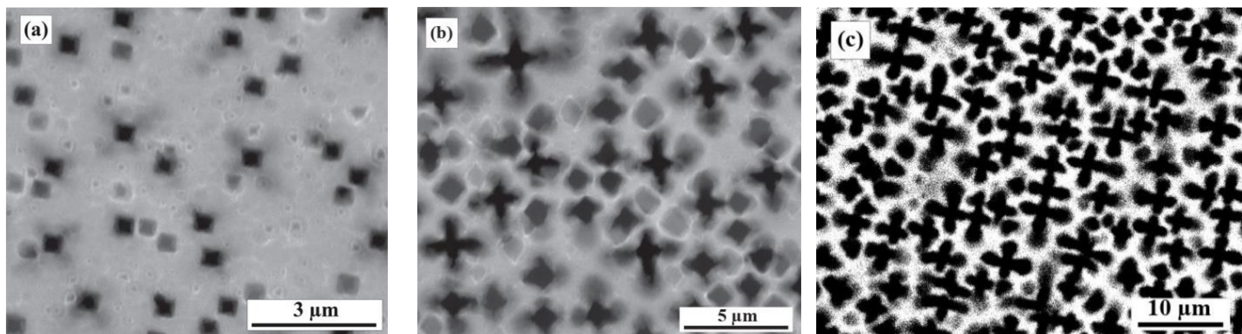

Figure 2: *SEM images of MPS (with H_2O_2) with etching time of (a) 10 (b) 20 and (c) 30 min.*

The length of square pore is 0.5µm and can be seen at different locations. Further increase of etching time from 10 min. (Sample a) to 20 min (sample b) causes the adjacent pores to breakdown and lead to the formation of connected four branch shaped pores with dimension of 2µm. According to a study published by Lehmann et al. [8], holes in the Si substrate may have enough energy to permeate into the branches in longer etching period, causing more dissolving and therefore enlarging the pores. However, significant changes of macropores morphology were observed as the etching time was increased to 30 min, extremely connected four branches shaped macropores with dimension of 6 µm were obtained. At this stage, the branches of adjacent macropores seem to connect to each other. A highly increase in the density of the connected branches, resulting in the increase of surface roughness, is observed. Figure 3 (a, b and c) shows the cross-sectional view SEM images of the MPS samples.

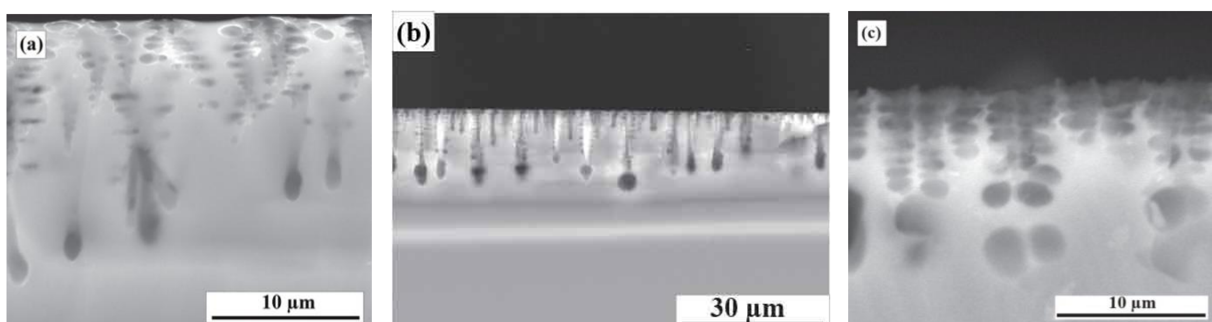

Figure 3: *SEM images of the cross-sectional view of MPS with the etching time of (a) 10 (b) 20 and (c) 30 min.*

As a general trend, different types of branched macropores have been observed. At 10- and 20-min etching process, the cleaved etched silicon samples (a, b) reveal thinner dendritic branched macropores with lengths of 12 and 5.85 µm, respectively. However, further etching time causes a change in the macropores morphology. The cross-sectional view of sample (c) indicates shorter and thick pores with lengths of 12 µm. This was expected, since larger pore sizes (which correspond to longer etch times) are less likely to branch [29]. Shorter etching time is thought to cause significant pore formation, which is ascribed to fluoride ions attacking Si-Si bonds (Si back bonds) directly as reported by several [30]. Different dissolving mechanisms begin to dominate as the etching time increases [31]. The pore wall is attacked, and the response at the pore tips is suppressed. As a result, the etching rate at the pore tip is slightly reduced.

Figure 4 shows the FTIR spectra of untreated silicon and MPS samples etched for (a) 10, (b) 20 and (c) 30 min. The reference spectrum of untreated silicon (Fig.4. curve (a)) has an intense bond around 611cm^{-1}, which corresponds to the stretching vibrations of the Si-Si and Si-C bonds combined, the stretching vibrations of

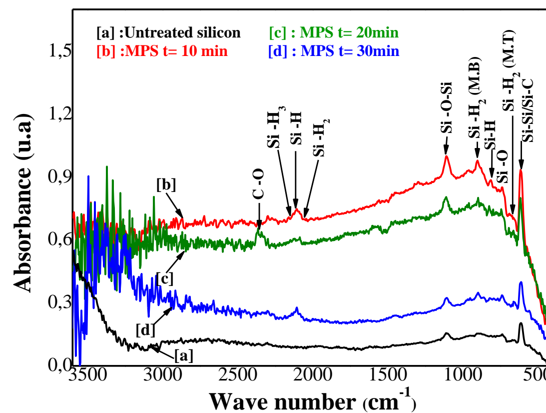

Figure 4: *FTIR spectra of (a) untreated silicon and MPS (with H_2O_2) etched at different times (b) 10 (c) 20 and (d) 30 min.*

the Si-O bonds are characterized by the peak at 729 cm^{-1} [32] . The absorption bands at 663 and 902cm^{-1} is assigned to Si-H_2 species bonding modes and stretching modes respectively [32]. Another absorption peak at 815 cm^{-1} illustrated the deformation vibration of the Si-H bond. The broad absorbing peak appearing at 1110cm^{-1} is attributed to the stretching vibration modes of Si-O-Si bonds [32], [33]. Furthermore, the anodized samples (Figs.4, curves (a),(b) and (c)) show absorption bands in stretching modes at 2084 cm^{-1}, 2109 cm^{-1} and 2139 cm^{-1} which are related to Si-H, Si-H_2 and Si-H_3, respectively [32].The spectra indicated a noticeable evolution of Si-H stretching (2084 cm^{-1}) and scissoring (815 cm^{-1}) modes by increasing the etching time. In addition, absorption peak at 2359 cm^{-1} corresponds to CO_2, probably caused by contamination of Si the surface in air [32].

The integrated IR areas under the SiH_x peaks of IR absorbance spectra (Fig.5), correlated with SiH_x species concentration shows that the concentration of SiH_x concentration increases first, stabilizes at about 10 min. etching time then decreases. It is clear from the figure that the maximum concentration of SiH_x species is observed for etching time 10-15 min. As the etching time is increased to 30 min, the pore size increases leading to the formation of branched pores as a consequence the crystallites surrounding the pores (SiH_x) are dissolved inducing the decrease of the Si-Hx species observed in Fig.5 [32], [34].

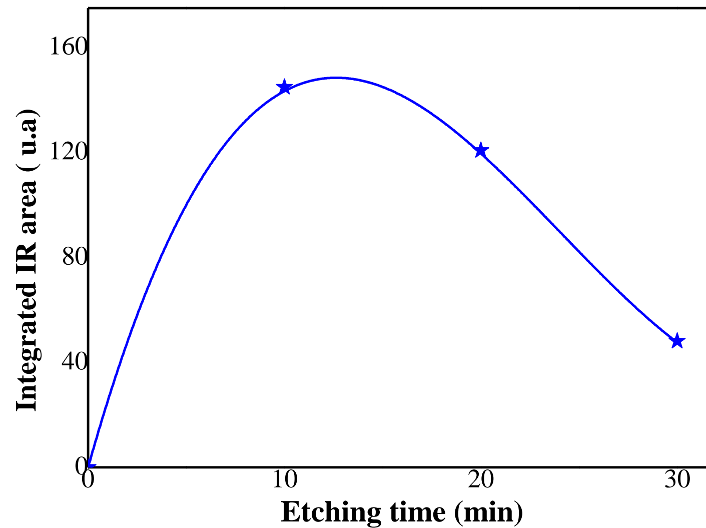

Figure 5: *Integrated IR area of SiH_x species calculated from Fig.4*

The porosity of the MPS was estimated by gravimetry method. In this process the porous layer was removed using a sodium hydroxide (99.95%) and deionized water solution in a ratio of 1:100, respectively, in which the PS was immersed, and the porous layer is removed during contact with this solution. The porosity was calculated by means of the following equation [26]:

$$P = (m_1-m_2)/(m_1-m_3) \quad (1)$$

Where, m_1 is the mass of the wafer of c-Si before the attack, m_2 is the mass of the wafer after the anodization, and m_3 is the mass of the same wafer after removing the MPS layer. The porosity percentages of the macroporous samples, as shown in Figure 6, calculated for 5-, 10-, 20- and 30-min. etching times were found 61 %, 74,91%, 70,22% and 65,81%, respectively. It is clear from Fig.6 that the porosity is increased by increasing the etching time, reaches a maximum porosity at about 10 min anodization time and then it decreases.

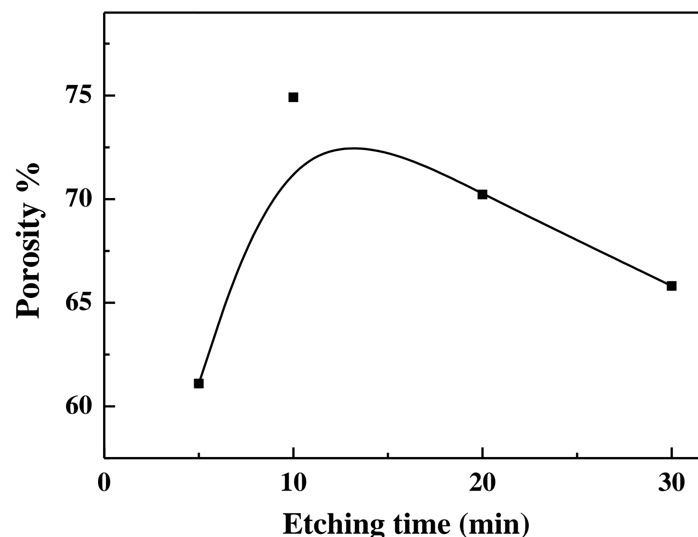

Figure 6: *Variation of the porosity as a function of the anodizing time*.

For the first part of the curve of Fig.6, this behavior can be explained by the fact that during etching the pore size increases, leading to a broadening of size distributions as reported by Herino et al. [26]. The decrease in MPS porosity can be correlated with the attack of the pore wall as commented on Fig.3 [30]. As

a consequence, the pore walls are attacked which enlarge the pore diameter diminishing the porosity of the samples.

Contact angle measurements can offer a good indication of the hydrophobic (or hydrophilic) nature of the sample surface. The difference in the value of this parameter is ascribed to the interaction between the liquid (DI) and the chemistry of the substrate surface. Hydrophobic surfaces are characterized by water-repellency, with water droplets residing on the surface exhibiting a contact angle higher than 90° and superhydrophobic surfaces with contact angles greater than 150°. The contact angle measurements of the silicon surface samples etched for 10, 20, and 30 min are displayed in figures 7 (a), (b), and (c), respectively. Our results show that increasing the etching times of the structures causes the water contact angle to increase, as shown in table1. The contact angle of the water on the MPS being greater than 90° and close to 150° which confirms the (super) hydrophobicity of this material. This behavior is in good agreement with other reported works[35], [36].

Table 1: *The contact angle of the water on the MPS*

Etching time (min)	10	20	30
Contact angle (°)	117.7	129.8	146.3

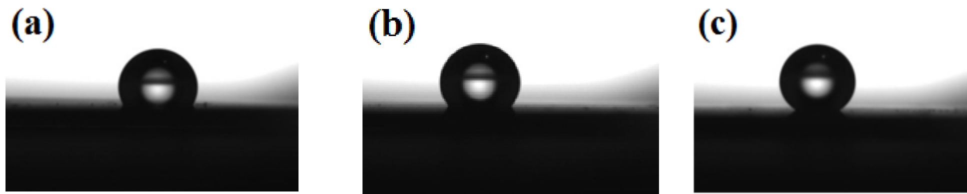

Figure 7: *Contact angle of MPS samples etched at (a) 10 min (b) 20 min and (c) 30 min*

Figure 8 shows the reflectivity of the three MPS samples etched for different etching time in the wavelength range from 400 to 2500 nm. It shows that intensity of the reflectivity of the MPS samples decreases as the etching time is raised. The reduction in reflectivity is due to trapping of light in the connected four branches shaped macropores layer as shown in Fig.2(c) [37]. The interference fringes observed on the spectra (Fig.8) are due essentially to the presence of pores and the roughness of the surface of the MPS layer. The thickness of the porous layer influences the amplitude of the reflection fringes.

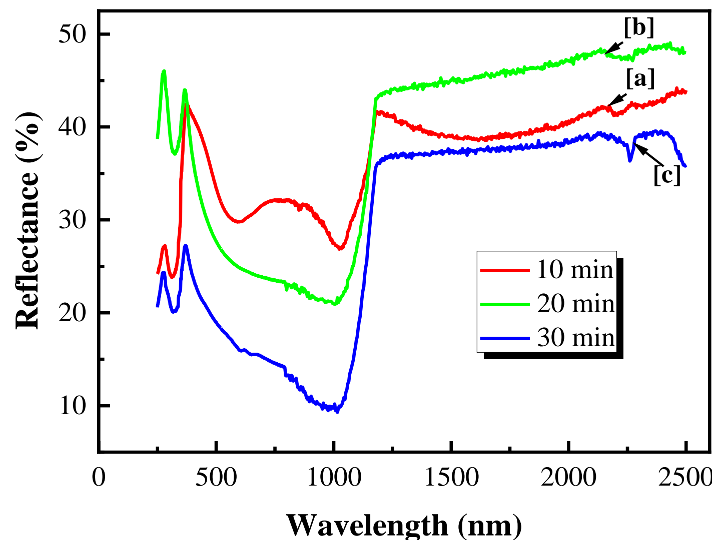

Figure 8: *Reflectance spectra of MPS etched at (a) 10 (b) 20 and (c) 30 min.*

4 Conclusion

This work was focused on the macropores formation on n-Si (100) using front-side illumination using two electrolytes the first one is composed of HF/Ethanol and the second containing an oxidizing agent H_2O_2. It is found that the introduction of H_2O_2 in the solution modifies the macropores morphology obtained. Square macropores are obtained in HF/Ethanol but enlarged and branched macropores are observed by adding H_2O_2. The pore size increases as the etching time increases. The behavior has been explained by the attack of the pore wall diminishing its passivation (observed by the decrease of SiH_x bonds) and then reducing slightly the etching rate at the pore tip.

5 Declarations

5.1 Competing Interests

The authors declare that there is no conflict of interests regarding the publication of this paper.

5.2 Publisher's Note

AIJR remains neutral with regard to jurisdictional claims in published institutional affiliations.

How to Cite this Article:

K. M'hammedi and N. Gabouze, "The Influence of Preparation Parameters on Structural and Optical Properties of N-Type Porous Silicon", *J. Mod. Mater.*, vol. 10, no. 1, pp. 3–10, Mar. 2023. https://doi.org/10.21467/jmm.10.1.3-10

References

[1] K. Isakov *et al.*, "Grass-like alumina nanoelectrodes for hierarchical porous silicon supercapacitors," *Energy Advances*, vol. 1, no. 12, pp. 1041–1050, Dec. 2022, doi: 10.1039/D2YA00177B.

[2] J. Schilling, F. Müller, S. Matthias, R. B. Wehrspohn, U. Gösele, and K. Busch, "Three-dimensional photonic crystals based on macroporous silicon with modulated pore diameter," *Appl Phys Lett*, vol. 78, no. 9, p. 1180, Feb. 2001, doi: 10.1063/1.1351533.

[3] H. Föll, J. Grabmaier, and V. Lehmann, "Process for producing crystalline silicon bodies having a structure which increases the surface area, and use of said bodies as substrates for solar cells and catalysts," DE3324232A1, Jul. 05, 1983 Accessed: Jan. 17, 2023. [Online]. Available: https://patents.google.com/patent/DE3324232A1/en

[4] S. R. Nicewarner-Peña *et al.*, "Submicrometer Metallic Barcodes," *Science (1979)*, vol. 294, no. 5540, pp. 137–141, Oct. 2001, doi: 10.1126/SCIENCE.294.5540.137.

[5] X.-L. Liu, Y. Zhao, L. Zhao, L. Zhao, J. Zhuang, and J. Zhuang, "Light-enhanced room-temperature gas sensing performance of femtosecond-laser structured silicon after natural aging," *Optics Express, Vol. 28, Issue 5, pp. 7237-7244*, vol. 28, no. 5, pp. 7237–7244, Mar. 2020, doi: 10.1364/OE.377244.

[6] G. Gautier, S. Kouassi, S. Desplobain, and L. Ventura, "Macroporous silicon hydrogen diffusion layers for micro-fuel cells: From planar to 3D structures," *Microelectron Eng*, vol. 90, pp. 79–82, Feb. 2012, doi: 10.1016/J.MEE.2011.04.003.

[7] D. H. Everett, "Manual of Symbols and Terminology for Physicochemical Quantities and Units, Appendix II: Definitions, Terminology and Symbols in Colloid and Surface Chemistry," *Pure and Applied Chemistry*, vol. 31, no. 4, pp. 577–638, Jan. 2019, doi: 10.1351/PAC197231040577

[8] V. Lehmann and S. Ronnebeck, "The Physics of Macropore Formation in Low-Doped p-Type Silicon," *J Electrochem Soc*, vol. 146, no. 8, pp. 2968–2975, Aug. 1999, doi: 10.1149/1.1392037

[9] V. Lehmann, "The Physics of Macropore Formation in Low Doped n-Type Silicon," *J Electrochem Soc*, vol. 140, no. 10, pp. 2836–2843, Oct. 1993, doi: 10.1149/1.2220919

[10] V. Lehmann and H. Föll, "Formation Mechanism and Properties of Electrochemically Etched Trenches in n-Type Silicon," *J Electrochem Soc*, vol. 137, no. 2, pp. 653–659, Feb. 1990, doi: 10.1149/1.2086525

[11] A. Rodríguez, D. Vega, R. Najar, and M. Pina, "Novel electronic devices in macroporous silicon: Design of FET transistors for power applications," *IEEE Trans Electron Devices*, vol. 58, no. 9, pp. 3065–3071, Sep. 2011, doi: 10.1109/TED.2011.2159508.

[12] D. S. García, D. C. Maza, Á. R. Martínez, and J. Llorca, "Absorption mechanisms in macroporous silicon photonic crystals," *Sens Actuators A Phys*, vol. 303, p. 111698, Mar. 2020, doi: 10.1016/J.SNA.2019.111698.

[13] L. A. Karachevtseva, M. T. Kartel, W. Bo, O. O. Lytvynenko, M. I. Karas, and V. F. Onyshchenko, "Creation of bilateral structures of macroporous silicon with nanocoatings for solar cells," *Surface Chemistry, Physics and Technology*, vol. 12, no. 2, pp. 90–97, 2021, doi: 10.15407/HFTP12.02.090.

[14] L. Calabrese, D. Palamara, E. Piperopoulos, E. Mastronardo, C. Milone, and E. Proverbio, "Deviceful LiCl salt hydrate confinement into a macroporous silicone foam for low-temperature heat storage application," *Journal of Science: Advanced Materials and Devices*, vol. 7, no. 3, p. 100463, Sep. 2022, doi: 10.1016/J.JSAMD.2022.100463.

[15] E. López, A. Irigoyen, T. Trifonov, A. Rodríguez, and J. Llorca, "A million-channel reformer on a fingertip: Moving down the scale in hydrogen production," *Int J Hydrogen Energy*, vol. 35, no. 8, pp. 3472–3479, Apr. 2010, doi: 10.1016/J.IJHYDENE.2010.01.146.

[16] J. A. Lewis and G. M. Gratson, "Direct writing in three dimensions," *Materials Today*, vol. 7, no. 7–8, pp. 32–39, Jul. 2004, doi: 10.1016/S1369-7021(04)00344-X.

[17] É. Vázsonyi *et al.*, “Porous silicon formation by stain etching,” *Thin Solid Films*, vol. 388, no. 1–2, pp. 295–302, Jun. 2001, doi: 10.1016/S0040-6090(00)01816-2.

[18] Z. Huang, N. Geyer, P. Werner, J. de Boor, and U. Gösele, “Metal-Assisted Chemical Etching of Silicon: A Review,” *Advanced Materials*, vol. 23, no. 2, pp. 285–308, Jan. 2011, doi: 10.1002/ADMA.201001784.

[19] M. Qi *et al.*, “A three-dimensional optical photonic crystal with designed point defects,” *Nature 2004 429:6991*, vol. 429, no. 6991, pp. 538–542, Jun. 2004, doi: 10.1038/nature02575.

[20] D. George *et al.*, “Holographic fabrication of 3D photonic crystals through interference of multi-beams with 4 + 1, 5 + 1 and 6 + 1 configurations,” *Optics Express, Vol. 22, Issue 19, pp. 22421-22431*, vol. 22, no. 19, pp. 22421–22431, Sep. 2014, doi: 10.1364/OE.22.022421.

[21] X. Gu, I. Gunkelk, and T. P. Russell, “Pattern transfer using block copolymers,” *Philosophical Transactions of the Royal Society A: Mathematical, Physical and Engineering Sciences*, vol. 371, no. 2000, Oct. 2013, doi: 10.1098/RSTA.2012.0306.

[22] M. A. Summers, K. Tabunshchyk, A. Kovalenko, and M. J. Brett, “Fabrication of 2D–3D photonic crystal heterostructures by glancing angle deposition,” *Photonics Nanostruct*, vol. 7, no. 2, pp. 76–84, May 2009, doi: 10.1016/J.PHOTONICS.2008.12.001.

[23] N. Gabouze and F. Ozanam, “Macroporous silicon,” in *Handbook of Porous Silicon*, Springer International Publishing, 2014, pp. 103–113. doi: 10.1007/978-3-319-05744-6_10

[24] R. Outemzabet, N. Gabouze, N. Kesri, and H. Cheraga, “Random macropore formation in n-type silicon under front side illumination: correlation with anisotropic etching,” *physica status solidi (c)*, vol. 2, no. 9, pp. 3394–3398, Jun. 2005, doi: 10.1002/PSSC.200461185.

[25] V. Depauw, H. J. Kim, G. Beaucarne, J. Poortmans, J. P. Celis, and R. Mertens, “Anodisation of branched and columnar macropores in n-type silicon under front-side illumination,” *physica status solidi c*, vol. 4, no. 6, pp. 1928–1932, May 2007, doi: 10.1002/PSSC.200674330.

[26] F. Severiano, G. García, L. Castañeda, M. Salazar Villanueva, and J. F. Méndez, “Importance of the electrolyte in obtaining porous silicon and how it modifies the optical and structural proprieties: Optical and microstructural investigation,” *J Nanomater*, vol. 2015, 2015, doi: 10.1155/2015/942786.

[27] L. Lu, W. Li, L. Zhang, and D. Ge, “Effects of Electrochemical Etching Conditions on the Formation and Photoluminescence Properties of P-Type Porous Silicon,” *IOP Conf Ser Mater Sci Eng*, vol. 484, no. 1, p. 012001, Mar. 2019, doi: 10.1088/1757-899X/484/1/012001.

[28] S. N. Sharma, R. K. Sharma, and S. T. Lakshmikumar, “Role of an electrolyte and substrate on the stability of porous silicon,” *Physica E Low Dimens Syst Nanostruct*, vol. 28, no. 3, pp. 264–272, Aug. 2005, doi: 10.1016/J.PHYSE.2005.03.020.

[29] V. Lehmann, B. Jobst, T. Muschik, A. Kux, and V. Petrova-Koch, “Correlation between optical properties and crystallite size in porous silicon,” *Jpn J Appl Phys*, vol. 32, no. 5 R, pp. 2095–2099, May 1993, doi: 10.1143/JJAP.32.2095

[30] C. Gondek, M. Lippold, I. Röver, K. Bohmhammel, and E. Kroke, “Etching silicon with hf-h2o2-based mixtures: Reactivity studies and surface investigations,” *Journal of Physical Chemistry C*, vol. 118, no. 4, pp. 2044–2051, Jan. 2014, doi: 10.1021/JP4105757

[31] J. Carstensen, M. Christophersen, and H. Foil, “Pore formation mechanisms for the Si-HF system,” *Materials Science and Engineering: B*, vol. 69–70, pp. 23–28, Jan. 2000, doi: 10.1016/S0921-5107(99)00287-1.

[32] A. Teyssot, A. Fidélis, S. Fellah, F. Ozanam, and J. N. Chazalviel, “Anodic grafting of organic groups on the silicon surface,” *Electrochim Acta*, vol. 47, no. 16, pp. 2565–2571, Jun. 2002, doi: 10.1016/S0013-4686(02)00116-0.

[33] X. Geng, M. Li, L. Zhao, and P. W. Bohn, “Metal-assisted chemical etching using Tollen’s reagent to deposit silver nanoparticle catalysts for fabrication of quasi-ordered silicon micro/nanostructures,” *J Electron Mater*, vol. 40, no. 12, pp. 2480–2485, Dec. 2011, doi: 10.1007/S11664-011-1771-1

[34] R. Suryana and N. Q. Aini, “Analysis of Porous Silicon Formation on N-type Si (100) using Laser-Assisted Electrochemical Anodization Method,” *Journal of Physics and Its Applications*, vol. 4, no. 2, pp. 28–32, May 2022, doi: 10.14710/JPA.V4I2.12664.

[35] G. Acikbas and N. Calis Acikbas, “Copper oxide- and copper-modified antibacterial ceramic surfaces,” *Journal of the American Ceramic Society*, vol. 105, no. 2, pp. 873–887, Feb. 2022, doi: 10.1111/JACE.18149.

[36] S. Ouir *et al.*, “Structural, morphological and optical characterization of CuO/ZnO nanocomposite films,” *Appl Phys A Mater Sci Process*, vol. 129, no. 1, pp. 1–10, Jan. 2023, doi: 10.1007/S00339-022-06277-3

[37] A.-M. Mouafki *et al.*, “Porous Silicon Antireflective Coatings for Silicon Solar Cells,” *Engineering, Technology & Applied Science Research*, vol. 12, no. 2, pp. 8354–8358, Apr. 2022, doi: 10.48084/ETASR.4803.

Publish your research article in AIJR journals-

- Online Submission and Tracking
- Peer-Reviewed
- Rapid decision
- Immediate Publication after acceptance
- Articles freely available online
- Retain full copyright of your article.

Submit your article at journals.aijr.org

Publish your books with AIJR publisher-

- Publish with ISBN and DOI.
- Publish Thesis/Dissertation as Monograph.
- Publish Book Monograph.
- Publish Edited Volume/ Book.
- Publish Conference Proceedings
- Retain full copyright of your books.

Submit your manuscript at books.aijr.org